Validation of Heating 7.2 Simulations Using Hot Box Test Data for RASTRA Wall Form System with Expanded Polystyrene–Beads
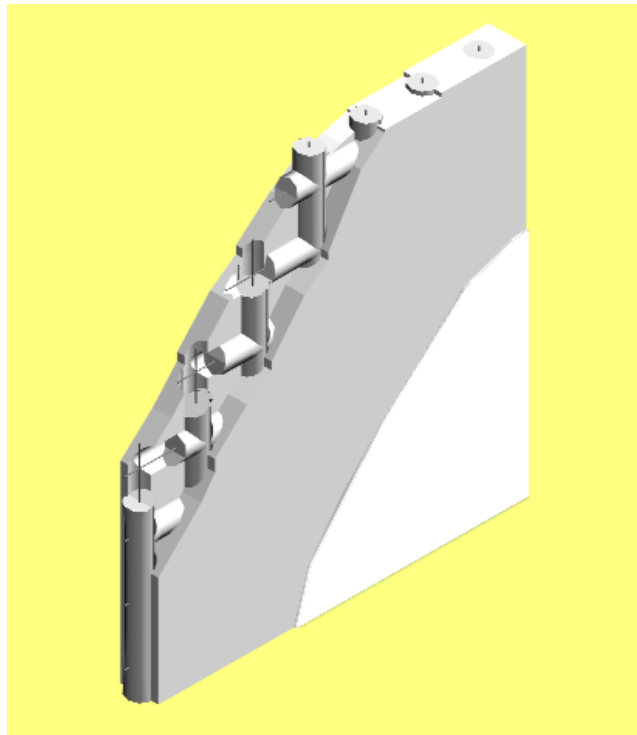
Jan Ko ny and Phill Childs

Oak Ridge National Laboratory
Buildings Technology Center

December 5, 2000

Introduction

Thermal performance of the Rastra wall system was measured in the Oak Ridge National Laboratory (ORNL) Buildings Technology Center (BTC) rotatable guarded hot box.. Hot-box test and finite difference computer modeling were used to analyze dynamic thermal performance of the clear wall area for the Rastra wall systems with 10-in.-thick expanded polystyrene (EPS)–bead concrete forms. Guarded hot-box tests formed the basis for a finite difference computer model calibration. Three-dimensional computer modeling enabled analysis of the temperature distribution in the wall and precise calculation of local heat fluxes in the clear wall area. Maps of the temperature distribution in the wall were developed. These maps were used to estimate the areas affected by the existing thermal bridges and to calculate R-values for these areas.

Description of the Rastra Wall

The Rastra wall system is based on 10-in.-thick, light-weight concrete forms filled with high-density, reinforced structural concrete. Wall forms are made of light-weight, EPS-bead concrete with a density of ~20 to 30 lb/ft^3. Detailed drawings of the Rastra wall components are presented Figures1. Normally, the Rastra wall is covered by light-weight stucco on the outside and plaster on the inside. For the hot-box tests, an unfinished wall was used as shown in Figure 2.
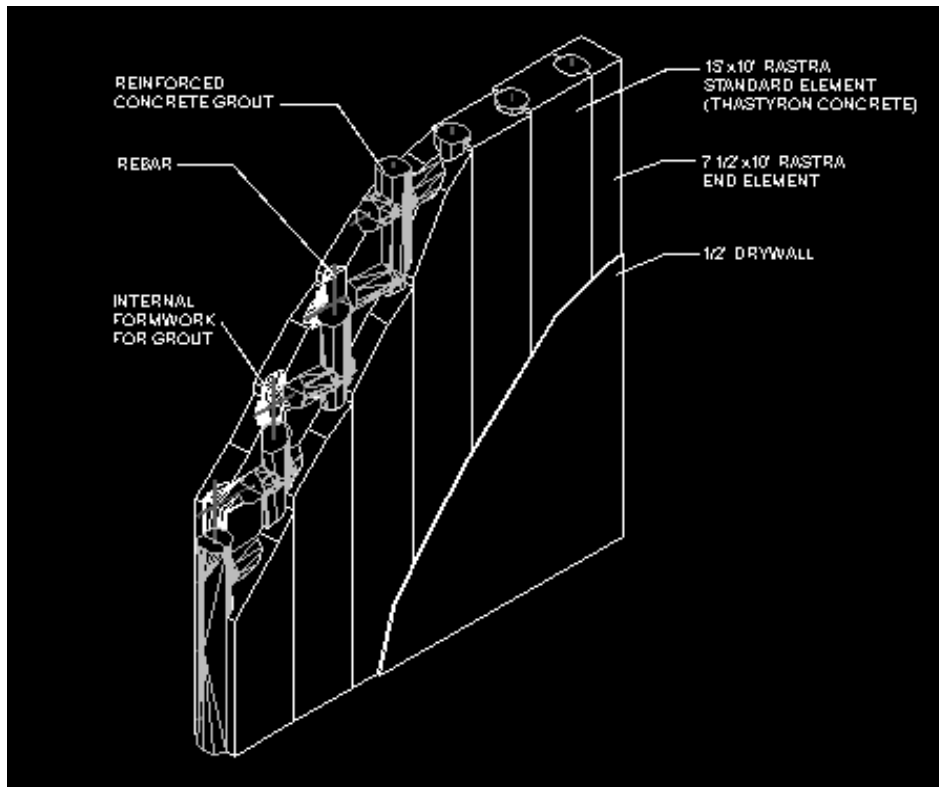
Figure 1. Rastra wall system - clear wall area (R-value = 7.61 hft^{2}F/Btu)
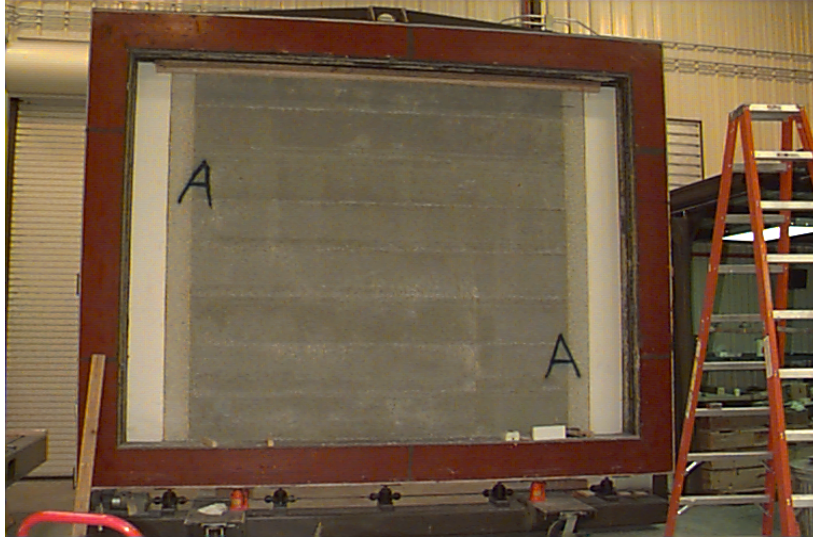
Figure 2. Unfinished Rastra wall prepared for hot-box test.

Guarded Hot-Box Thermal Test of the Rastra Wall

Measurements of wall systems are typically carried out by apparatus such as the one described in ASTM C236-89, "Standard Test Method for Steady-State Thermal Performance of Building Assemblies by Means of a Guarded Hot Box [ASTM 1993]." A relatively large (~8 ft^2 or larger) cross section of the clear wall area of the wall system is used to determine its thermal performance. The precision of this test method is reported to be ~8% [ASTM 1993]. The calibration of the ORNL BTC guarded hot box is described in Appendix A.

At the ORNL BTC, the Rastra wall was built and tested in a guarded hot box under steady-state and dynamic conditions. Experimental data recorded during the hot-box test are presented in Figures 3 through 7.

Meter Chamber Temperatures
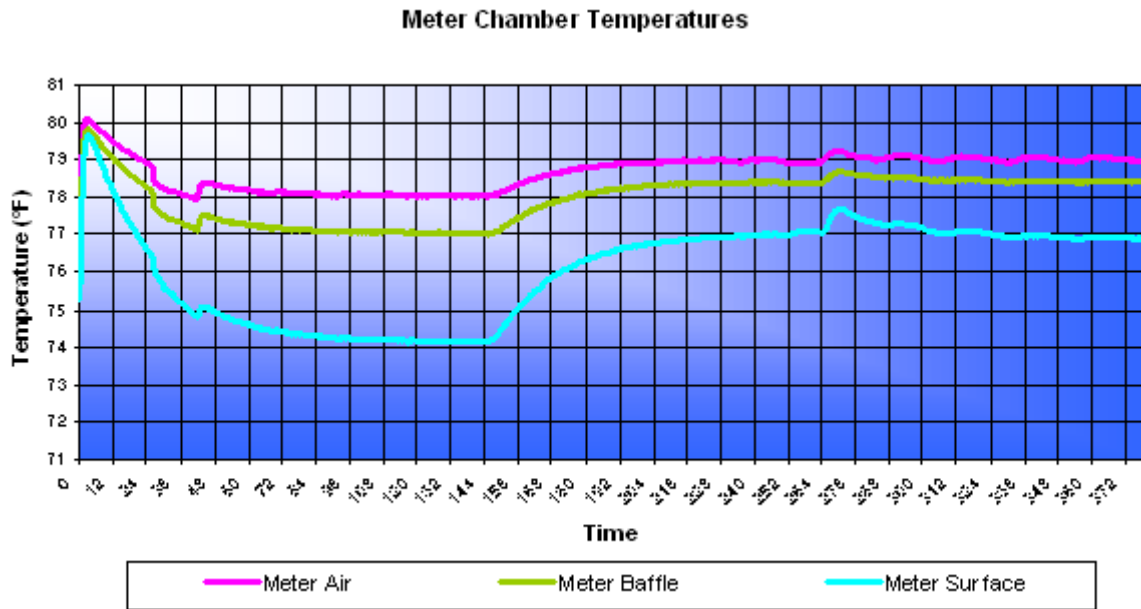
Figure 3. Meter-side temperatures for Rastra wall during hot-box test.

Climate Chamber Temperatures
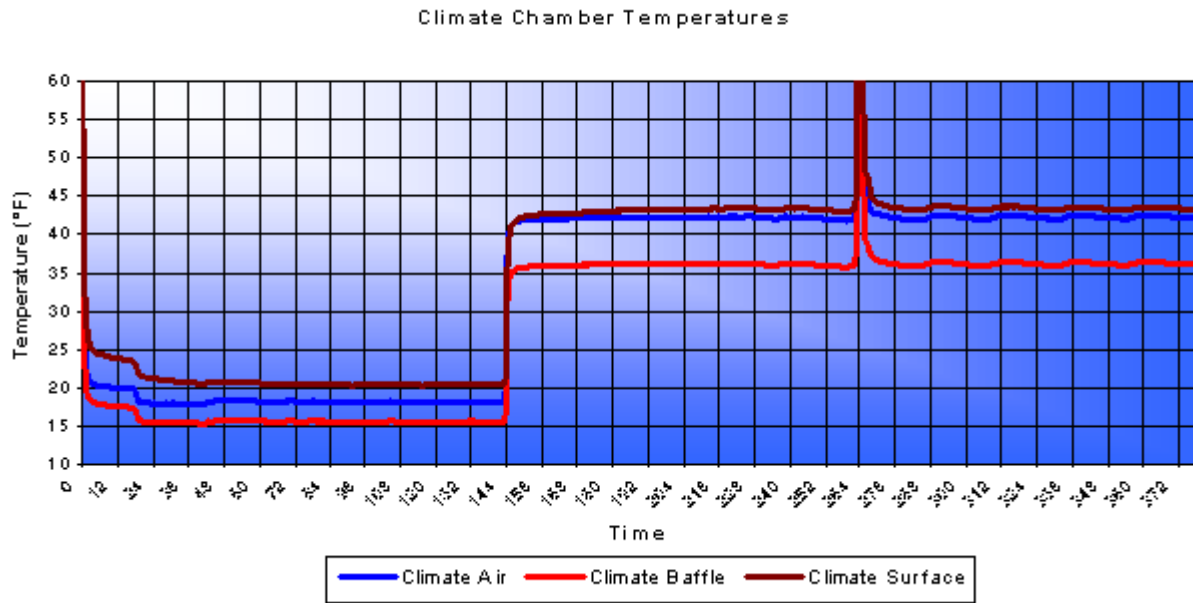
Figure 4. Climate-side temperatures for Rastra wall during hot-box test.

**Temperature Difference
Meter-Climate**
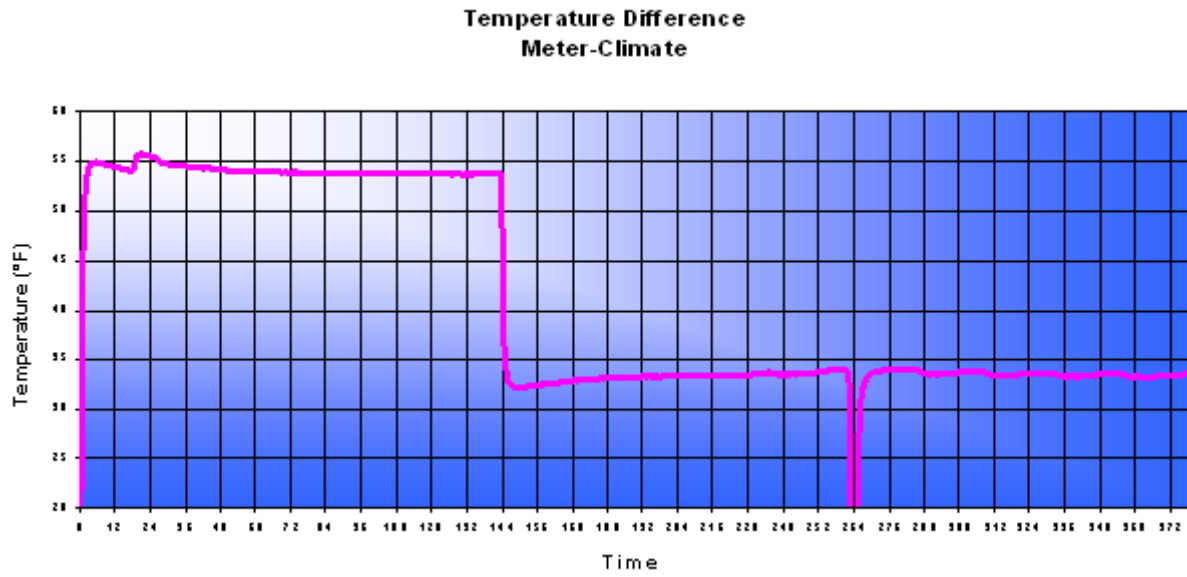
Figure 5. Temperature differences between climate and meter side of Rastra wall during hot-box test.
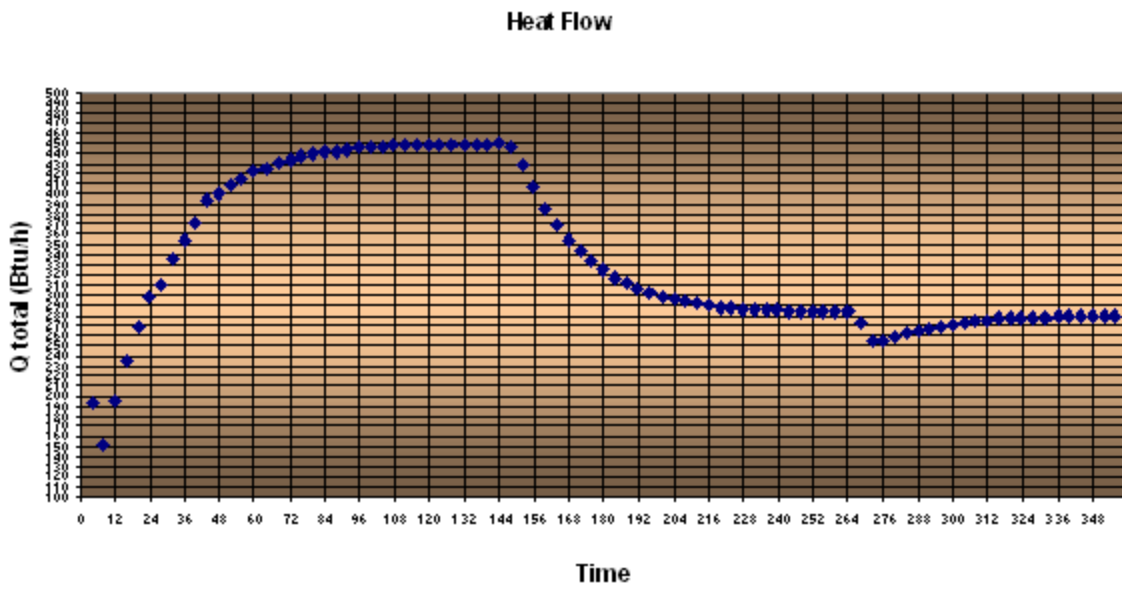
Heat Flow

Figure 6. Heat flux for Rastra wall measured during hot-box test.

Air Velocity Measurements
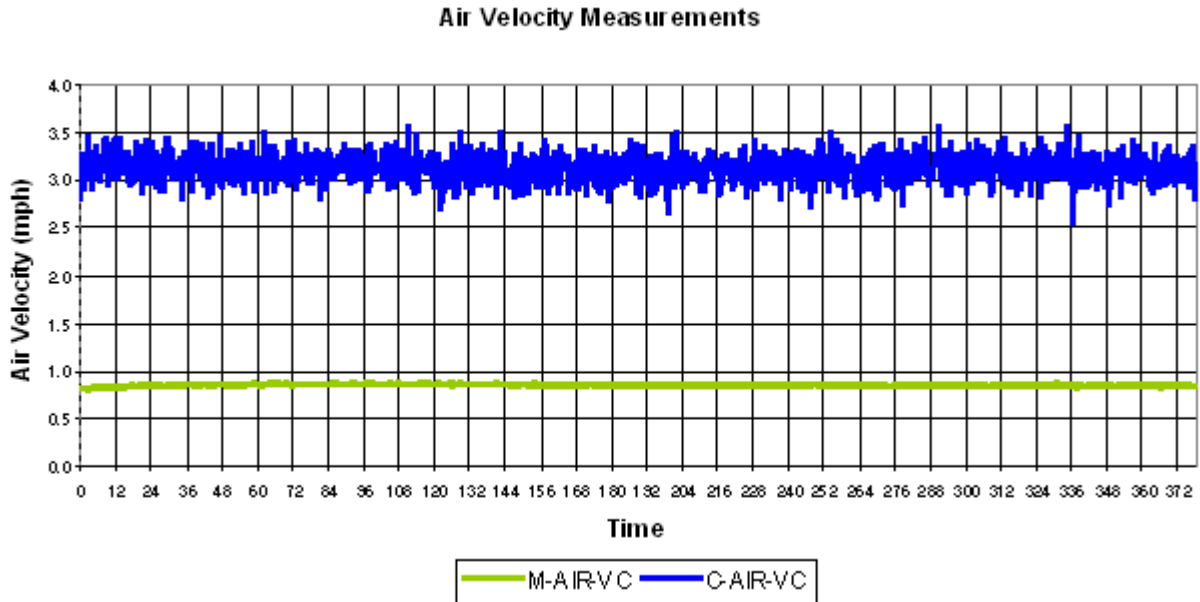
Figure 7. Air velocities for Rastra wall hot-box test.

As presented in Figures 3 and 4, two steady-state periods were achieved during the hot-box test. The meter-side temperature was kept relatively constant at ~79°F. The climate-side temperature was ~20°F during the first steady-state period and was later increased to ~40°F during the second period. Dynamic change of temperatures is later used for dynamic thermal performance analysis.

Figures 3 through 7 depict the experimental data compiled during the hot-box testing. The temperature data presented previously enable calculation of the average temperature for the time interval after steady state was achieved.

The surface-to-surface thermal resistance (R-Value) is calculated by

$$R = \frac{A(t_1 - t_2)}{(Q_h + Q_f)} , \tag{1}$$

where

R = thermal resistance of wall assembly, h ft^2 °F/Btu (m^2 K/W);
A = area of metering chamber, 64 ft^2 (5.3 m^2);
t_1 = average surface temperature of wall assembly on metering side, °F (°C);
t_2 = average surface temperature of wall assembly on climate side, °F (°C);
Q_h = metering heater energy input, Btu/h (W);
Q_f = metering fan energy input, Btu/h (W).

The overall thermal resistance (R_u-value, which includes surface film resistances) is calculated by

$$R_u = \frac{A(t_h - t_c)}{(Q_h + Q_f)} \; , \tag{2}$$

where

R_u = overall thermal resistance of wall assembly, h ft^2 °F/Btu (m^2 K/W);
A = area of metering chamber, 64 ft^2 (5.3 m^2);
t_h = average meter-side air temperature, °F (°C);
t_c = average climate-side air temperature, °F (°C);
Q_h = metering heater energy input, Btu/h (W);
Q_f = metering fan energy input, Btu/h (W).

Figure 7, depicts climate- and meter-side air film thermal resistances. The meter-side air film thermal resistance ($R_{ms\,air}$) is calculated by

$$R_{ms\,air} = \frac{A(t_h - t_1)}{(Q_h + Q_f)} \; , \tag{3}$$

where

$R_{ms\,air}$ = meter-side film thermal resistance of wall assembly, h ft^2 °F/Btu (m^2 K/W);
A = area of metering chamber, 64 ft^2 (5.3 m^2);
t_h = average meter-side air temperature, °F (°C);
t_1 = average surface temperature of wall assembly on metering side, °F (°C);
Q_h = metering heater energy input, Btu/h (W);
Q_f = metering fan energy input, Btu/h (W).

The climate-side air film thermal resistance ($R_{cms\,air}$) is calculated by

$$R_{sc\,air} = \frac{A(t_2 - t_c)}{(Q_h + Q_f)} \; , \tag{4}$$

where

$R_{cs\,air}$ = climate-side film thermal resistance of wall assembly, h ft^2 °F/Btu (m^2 K/W);
A = area of metering chamber, 64 ft^2 (5.3 m^2);
t_2 = average surface temperature of wall assembly on climate side, °F (°C);
t_c = average climate-side air temperature, °F (°C);
Q_h = metering heater energy input, Btu/h (W);
Q_f = metering fan energy input, Btu/h (W).

Metering box wall losses were not included in any of the energy balance calculations. In the worst case, the metering box wall loss represents less than 0.2% of the energy input ($Q_h + Q_f$). The clear wall *steady-state R-value*, which was achieved during analysis of Rastra wall experimental results, is *7.68 h ft^2 °F/Btu.*

Thermal Analysis Method

Three-dimensional computer modeling was used for Rastra wall thermal performance study. A heat conduction, finite difference computer code, HEATING 7.2 [Childs 1993], was used for this analysis. The resultant isotherm maps were used to calculate average heat fluxes and wall system R-values. The capability of HEATING 7.2 to accurately predict wall system R-values was verified by comparing simulation results with published test results for 28 masonry, wood-frame, and metal-frame walls tested at other laboratories. The average differences between laboratory test and HEATING 7.2 simulation results for these walls were +/- 4.7% [Ko ny and Desjarlais 1994]. Considering that the precision of the guarded hot-box method is reported to be ~8%, the ability of HEATING 7.2 to reproduce the experimental data is within the accuracy of the test method [ASTM 1993].

The results of the ORNL BTC guarded hot-box test for the Rastra wall were used to calibrate the computer model of the Rastra wall. The Rastra wall was modeled using dimensions obtained from the test wall. Then, the results of the computer modeling were compared with R-values measured by the hot-box test. In this phase of thermal modeling, actual tested thermal properties of materials were used. Thermal conductivity of Rastra EPS-bead concrete material used in tests was measured in the ORNL Material Properties Laboratory using ASTM C518 procedure [ASTM 1991]. This material conductivity was used as an input to the finite difference computer code for calibration of the computer model. Also, it was found that this material is very sensitive to any changes in moisture content. That is why an additional set of the Rastra concrete ASTM C518-91 measurements were performed to find the relation between moisture content and thermal conductivity..

Calibration of the Computer Code and Steady-State Clear Wall Thermal Performance

Wall dimensions obtained from the test Rastra wall were used to develop a three-dimensional finite difference computer model. For the simulated wall, all material thermal properties were identical as measured on the samples received from the experimental Rastra wall. Thermal conductivity of Rastra concrete was measured in ORNL Material Properties Laboratory using ASTM C518-91 procedure.

HEATING 7.2 finite difference computer code was used to simulate the Rastra wall. Then, the results of the computer modeling were compared with hot-box experimental R-value measurements. This procedure enabled calibration of the computer model. Thermal conductivities for all wall materials used in computer modeling are presented in Table 1. Test and simulated R-values are within +/-1% of each other, as shown in Table 2.

Table 1. Thermal conductivities for all wall materials used
in calibration of the computer model

Material	Density lb/ft^3 [kg/m^3]	Conductivity k_a Btu-in./h ft^2 °F [W/mK]	Specific heat Btu/lbF [kJ/kgK]	Resistivity R/in., h ft^2 °F/Btu-in. [mK/W]
Rastra EPS-bead concrete	25.0 [400]*	0.87 [0.125]**	0.27 [1.13]***	1.15 [8.04]*
High-density concrete	120.0 [ ]	9.09 [1.30]	0.21 [0.88]	0.11 [0.77]

*As measured in the ORNL BTC after the hot-box test moisture content was about 5%.
**As measured in the ORNL Material Properties Laboratory using ASTM C518-91 procedure.
***Data provided by Rastra based on European test results.

Table 2. Comparison of hot-box measured R-values
with computer prediction results

Wall	ORNL Hot-Box Test R-value, h ft^2 °F/Btu [m^2 K/W]	Simulated R-value h ft^2 °F/Btu [m^2 K/W]	Difference %
Rastra wall	7.68 [1.35]	7.61 [1.34]	0.9
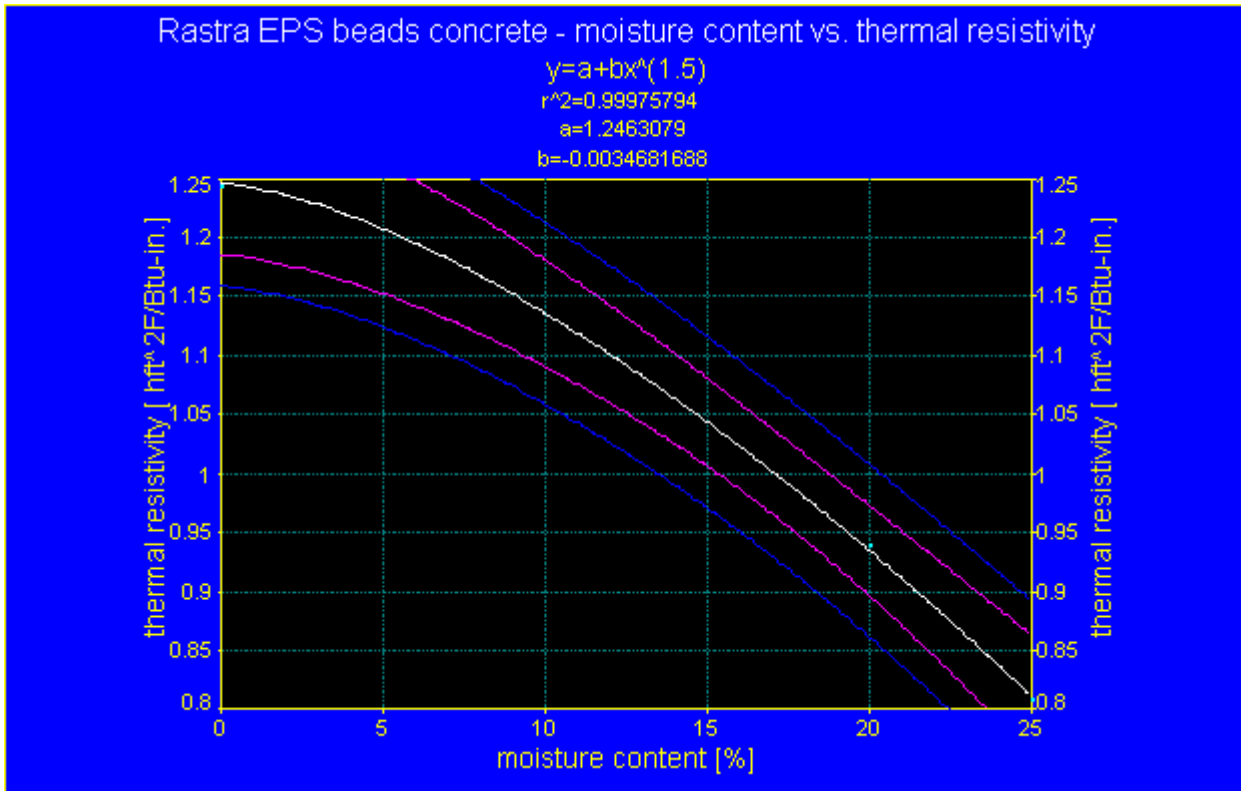
Figure 8. Regression analysis showing the relationship between moisture content and thermal resistivity for Rastra EPS-bead concrete based on ASTM C518-91 test results.

In addition, ORNL measured the thermal conductivity and moisture content of a set of samples made of EPS-bead concrete at a mean temperature of 75 F. ASTM C518-91 procedure was used [ASTM 1991]. Also, a small sample, ~5 × 5 × 2 in., was taken from the test wall just after completion of the hot-box test. The moisture content of this sample was ~5%. The results of ASTM C518-91 measurements are presented in Figure 8.

Dynamic Thermal Modeling of the Rastra Wall and Validation of Dynamic Model

Dynamic measurements of wall systems are typically carried out by an apparatus such as described in ASTM C236-89, "Standard Test Method for Steady-State Thermal Performance of Building Assemblies by Means of a Guarded Hot Box" [ASTM 1989]. A full-scale representative (8 ft^2) cross section of the clear wall area of the wall system is used to determine its dynamic thermal performance. A dynamic test typically consists of the three basic stages:

> steady-state stage (steady temperatures on both sides of the wall),
> thermal ramp (rapid change of the temperature on one side of the wall), and
> stabilizing stage (wall is kept under the second set of steady boundary temperatures until steady-state heat transfer occurs).

The precision of dynamic testing is close to the precision of the steady-state test method, which is reported to be ~8% [ASTM 1989]. The dynamic test results were used to calibrate the finite difference computer model used in the analytical part of this project.

At the ORNL BTC, a wall built with the Rastra 10-in.-thick, light-weight concrete forms was tested in the guarded hot box under dynamic conditions.

The dynamic response of the wall was analyzed for a 20°F thermal ramp (it took 2 hours to change the surface temperature on the climate side of the wall from 20 to 40°F). Temperatures on both sides of the wall were stabilized, and the experiment was continued until steady-state heat transfer occurred. During the first stage of the test process, air temperatures on both sides of the wall were stabilized at 80 and 20°F. During the second stage, the climate-side air temperature was increased from 20 to 40°F. Air temperatures for the meter and climate sides of the wall and measured heat flux on the meter chamber side of the wall are presented in Figures 3, 4, 5 and 6 in.

Validation of the developed computer model of the Rastra wall was made by comparing computer heat flow predictions to the hot-box measured heat flow through an 8-by-8-ft Rastra clear test wall exposed to dynamic boundary conditions. As shown in Figure 9, good agreement was found between test and computer modeling results.
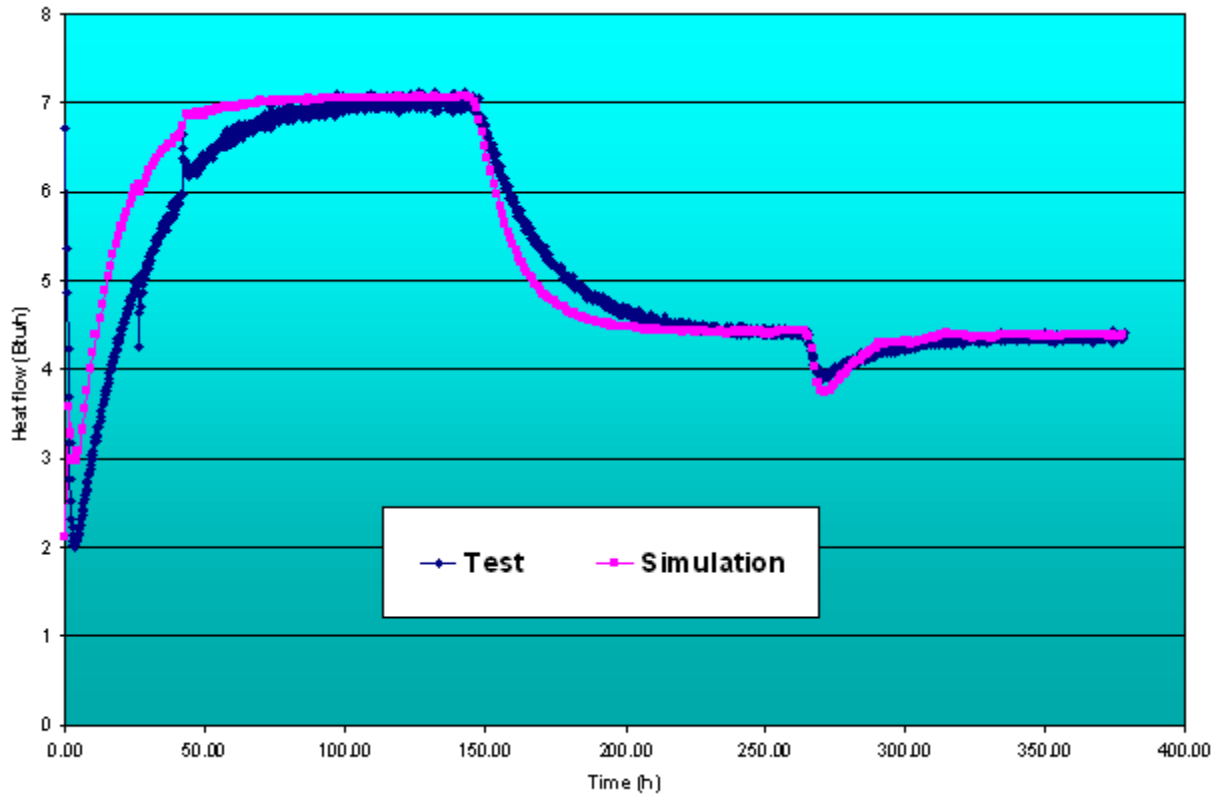
Figure 9. Comparison of measured heat flux against simulated heat flux for dynamic hot-box test of the Rastra wall.

Measured air temperatures; 6 in. away from the surface of the metering side and 14 in. away from the climate side, along with air velocities measured in the meter and climate chambers, were used as boundary conditions for dynamic modeling of the Rastra wall. The computer program, reproduced all recorded test boundary conditions (temperatures and heat transfer coefficients) with 1-hour time intervals. The Rastra wall internal geometry was numerically described to create the HEATING 7.2 input file. The following thermal properties of materials were used in calibration of the dynamic model:

thermal conductivity of Rastra light-weight concrete blocks, 0.87 Btu-in./h ft² °F,
thermal conductivity of core concrete, 9.09 Btu-in./h ft² °F.

Values of heat flux on the surface of the wall generated by the program were compared with the values measured during the dynamic test. As depicted in Figure 9, the computer program reproduced the test data very well. The average discrepancy between test-generated and simulated heat fluxes was less than 5% (the first 60 hours of the simulation were neglected because of the different initial conditions). This comparison confirms the ability of HEATING 7.2 to reproduce the dynamic heat transfer process measured during the dynamic hot-box testing of the actual Rastra wall.

Conclusions

Steady state hot-box tests and finite difference computer modeling were used to examine the steady-state thermal performance of the Rastra wall system. The *hot-box tested (ASTM C236-89) clear wall R-value for the Rastra wall system was 7.68 h   ft² °F/Btu.*

HEATING 7.2 finite difference computer code was used to simulate the Rastra wall. Then, the results of the computer modeling were compared with hot-box experimental R-value measurements. This procedure enabled calibration of the computer model. Test and simulated R-values are within +/-1% of each other.

Measured air temperatures, along with air velocities measured in the meter and climate chambers, were used as boundary conditions for dynamic modeling of the Rastra wall. The computer program, reproduced all recorded test boundary conditions (temperatures and heat transfer coefficients) with 1-hour time intervals. Values of heat flux on the surface of the wall generated by the program were compared with the values measured during the dynamic test. The average discrepancy between test-generated and simulated heat fluxes was less than 5% (the first 60 hours of the simulation were neglected because of the different initial conditions).

The above comparisons confirm the ability of HEATING 7.2 to reproduce the steady-state and dynamic heat transfer processes measured during the dynamic hot-box testing of the complex and massive wall structure.

References

ASTM 1991. Standard C518-91. "Standard Test Method for Steady-State Heat Flux Measurements and Thermal Transmission Properties by Means of the Heat Flow Meter Apparatus," Vol. 4.06, p. 153.

ASTM 1993. Standard C236-89. "Standard Test Method for Steady-State Thermal Performance of Building Assemblies by Means of a Guarded Hot Box," Vol. 4.06, ASTM, Conshohocken, Pa., pp. 53–63.

Childs, K. W. February 1993. *HEATING 7.2 Users' Manual*, ORNL/TM-12262, Oak Ridge Natl. Lab., Martin Marietta Energy Systems.

Christian, J., and Ko ny, J. March 1996. "Thermal Performance and Wall Rating," *ASHRAE Journal*, Atlanta.

Ko ny, J., and Desjarlais, A. O. July 1994. "Influence of Architectural Details on the Overall Thermal Performance of Residential Wall Systems," *Journal of Thermal Insulation and Building Envelopes*, Technomic Pub. Co., Lancaster, Pa.

Appendix A:

Hot Box Test Procedure

The wall assemblies were tested in accordance with ASTM C 236-89, "Steady-State Thermal Performance of Building Assemblies by Means of a Guarded Hot Box" using the Oak Ridge National Laboratory Rotatable Guarded Hot Box (RGHB). A photograph of the test facility is shown in Figure A1.
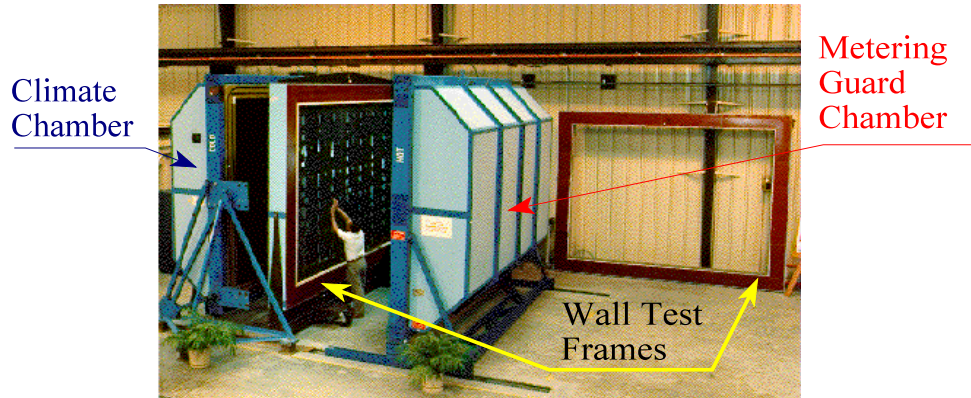
Figure A1. ORNL guarded hot box.

The test wall assemblies were installed into a specimen frame which is mounted on a moveable dolly. The specimen frame has an aperture of 4 by 3 m (13' 1" by 9' 10" ft.) -Figure A2.. Since the wall assemblies being evaluated are all smaller than this aperture, the remaining area is filled with a thermally resistive insulation material and the thickness of the fill material is adjusted to match the thickness of the test wall assembly. The specimen frame/test wall assembly is inserted between two chambers of identical cross-section.
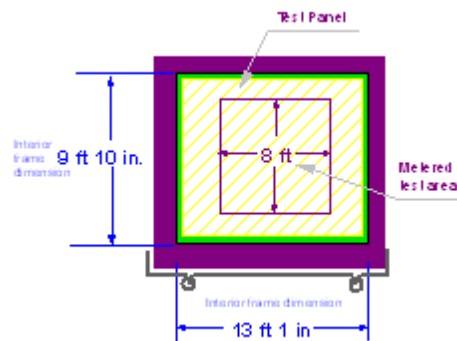
Figure A2. ORNL BTC Hot Box test panel schematic.

The insertion of the test wall assembly between the chambers allow the chamber temperatures to be independently controlled. These chambers are designated as the climate (cold) and metering/guard (hot) chambers.

In the climate chamber, a full-size baffle is mounted approximately 10 in. (250 mm) from the test wall assembly. Temperature control in this chamber is accomplished by the insertion of a refrigerated air and electrical resistance heaters in series with an array of air blowers. An external refrigeration system is operated continuously and cooled air is transferred from the refrigeration system through insulated flexible ducting into the rear of the climate chamber behind the baffle. Five centrifugal air blowers, installed in the climate chamber behind the baffle, are used to circulate the air through a bank of electrical resistance heaters and through the airspace between the baffle and test wall assembly. Temperature control is accomplished by a combination of controlling the airstream temperature entering the climate chamber and fine-tuning that temperature with the resistance heaters. The air velocity parallel to the climate side of the test wall assembly is controlled by adjusting the electric power input frequency to the air blowers. An anemometer continuously measures the wind speed in the airspace.
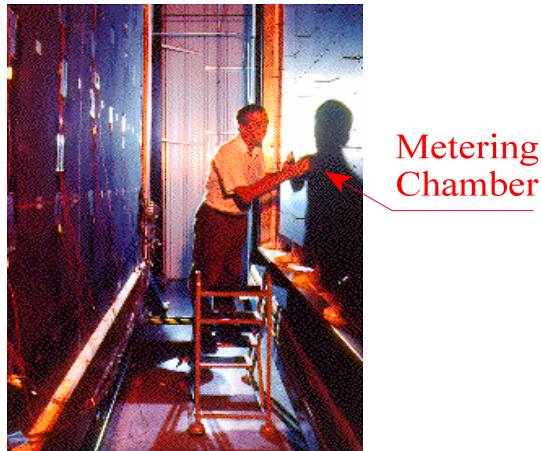
Metering Chamber

Figure A3. Metering chamber.

In the center of the metering/guard chamber, a metering chamber is pressed against the test wall assembly. A photograph of the metering chamber is shown in Figure A3. The metering chamber is approximately dimensioned 8 ft. (2.3 m) square by 1.3 ft. (0.4 m) deep. The walls of the metering chamber are constructed with 3-in. (76 mm) thick aged extruded polystyrene foam having an approximate thermal resistance of 15 hr ft^2 F/Btu (2.6 m^2 K/W) at 75 F (24 C). The walls of the metering chamber are reinforced with aluminum frames on the interior and exterior sides and are interconnected with fiberglass threaded rods. The edge of the metering chamber which contacts the test assembly is tapered to a thickness of 0.75-in. (19 mm) and a 0.5-in. (13 mm) square neoprene rubber gasket is affixed to this tapered edge. This gasket is very compressible and readily flows the couture of the test wall surface to minimize air leakage form the metering to the guard chamber. A baffle is mounted inside the metering chamber 6-in. (150 mm) from the exposed edge of the gasket. Behind the baffle, an array of eight fans and four electric resistance heaters are installed. These components are installed such that air is pulled downward behind the baffle, through the resistance heaters, and upward through the airspace

between the baffle and test assembly. The upper and lower rear corners of the metering box are tapered to minimize air impingement onto the metering box walls and to provide a smooth transition into the baffle space.

A ninety-six junction (forty-eight pair) differential thermopile is applied on the interior and exterior walls of the metering chamber to sense the temperature imbalance between the metering and guard chambers. Each thermopile junction is mounted in the center of equivalent surface areas; the interior junction is mounted directly opposite to the corresponding exterior junction. Four heaters and six fans are installed in the guard box to supply heat and circulate the air. These heaters and fans are situated to uniformly distribute the heat and not impinge directly onto the metering chamber.

All temperature measurements were performed using Type T copper/constantan thermocouples calibrated to the special limits of error specified in ASTM E 230, "Temperature-Electromotive Force (EMF) Tables for Standardized Thermocouples." All thermocouples were fabricated with No. 26 AWG wire prepared from the same spool. Arrays of thirty-six and forty-eight thermocouples were used to measure the meter and climate chamber air temperatures. Additional arrays of temperature sensors are affixed to each side of the test wall assembly to measure the surface temperature of each wall system component. All of the thermocouples that were attached to the surface of the test wall assemblies were affixed with duct tape. To determine the average surface temperature, the average temperature of the individual wall system components are area-weighted.

In operation, the temperature of the climate chamber is set at the desired level. A controllable AC source is used to energize the metering chamber heaters while the metering chamber fans are powered using a programmable D.C. power supply. The power to the fans is fixed to maintain the desired wind speed in the airspace between the baffle and the test wall assembly. An anemometer is used to set and monitor this wind speed. The power to the metering heaters is adjusted to obtain the required metering chamber air temperature. The output of the differential thermopile is used to energize the heaters in the guard chamber by using a differential temperature controller. By this technique, the temperature difference across the metering chamber walls could be minimized, thereby permitting negligible heat leaks into or out of the metering chamber.

These conditions are maintained until temperatures and heat flows equilibrated. The heat flow generated by the heaters is measured using a watt-hour transducer and the energy dissipated by the fans is metered with precision resistor networks. Once steady-state conditions have been achieved, the test period is continued until two successive four hour periods produce results that varied nonmonotonically by less than one percent. The data for each period is the average of one-minute scans for that period.

The thermal resistance is calculated by

$$R = \frac{A(t_1 - t_2)}{(Q_h + Q_f + Q_{mb})} \qquad \text{(A1)}$$

where   R   =   thermal resistance of wall assembly, hrft² F/Btu (m² K/
      A =   area of metering chamber, ft² (m²),
      t_1 =   average surface temperature of the wall assembly on the metering side, F
(C);
      t_2 =   average surface temperature of the wall assembly on the climate side, F
(C);
      Q_h =   metering heater energy input, Btu/hr (W);
      Q_f =   metering fan energy input, Btu/hr (W); and
      Q_{mb} =   metering chamber wall energy exchange between the metering and guard
chambers, Btu/hr (W).

To verify the performance of the rotatable guarded hot box, we performed a series of five verification experiments on a homogeneous panel comprised of a 5-in. (127 mm) thick expanded polystyrene foam core faced on both sides with 0.12-in. (3 mm) high impact polystyrene sheet. In these experiments, we varied the test conditions (temperatures of the metering and climate chambers) and the differential thermopile setting. These experiments were performed to assess how closely we needed to maintain the null balance of the thermopile and to determine the precision of the RGHB. A summary of these results is presented in Table A1.

The R-value data presented in Table A1 have already been corrected for any deliberate thermopile imbalance. The metering chamber input heat flow is corrected for any losses through the metering chamber walls to determine the specimen heat flow. The metering chamber wall heat flow was calculated by

$$Q_{mb} = \frac{A_{mb} * \Delta T_{mb}}{R_{mb}} \qquad \text{(A2)}$$

where Q_{mb} =   heat flow through metering chamber walls, Btu/hr (W);
      A_{mb} =   surface area of the metering chamber, ft² (m²);
      T_{mb} =   temperature imbalance across the metering chamber walls, F (C); and
      R_{mb} =   thermal resistance of the metering chamber walls, hr ft² F/Btu (m² K/W).

At mean temperatures of 50 and 75 F (10 and 24 C), the differential thermopile bias correction yields R-values that are within 0.05 and 0.02 hr ft² F/Btu (0.009 and 0.004 m²K/W) of the average values, respectively. To obtain a 10 Btu/hr (2.9 W) bias from the metering chamber requires a 1.5 F (0.8 C) temperature imbalance across the metering chamber walls.

In addition to testing the verification panel in the RGHB, specimens of the EPS foam used to fabricate the verification panel were submitted to the Materials Thermal Analysis Group at the Oak Ridge National Laboratory. They measured the thermal resistance of these specimens in accordance with ASTM C 518-91, "Steady-State Heat Flux and Thermal Transmission Properties by Means of a Heat Flow Meter Apparatus." Using handbook values for the thermal resistance of the polystyrene sheet (0.36 hr ft^2 F/Btu or R = 0.063 m^2 K/W) and adding this thermal resistance to the R-value of the EPS foam, the R-value vs. temperature for the specimen of the verification panel was determined. These data were linearly regressed and compared to the data compiled in the RGHB. Table A2 summarizes these results.

Table A1. Summary of experimental results obtained on the expanded polystyrene foam verification panel. The effects of mean temperature and differential thermopile balance are sought.

Test	Temperature				Heat Flow			R-value
	Meter F	Climate F	Mean F	Thermopile F	Input Btu/hr	Metering Box Btu/hr	Specimen Btu/hr	hr ft^2 F/Btu
1	98.9	52.3	75.6	-0.04	142.5	-0.3	142.2	21.14
2	98.8	52.7	75.7	-1.03	149.0	-6.9	142.1	21.14
3	99.0	51.1	75.0	0.87	135.3	5.8	141.1	21.16
4	96.6	4.6	50.6	-0.05	267.0	-0.3	266.7	22.07
5	97.5	6.6	52.0	0.87	258.7	5.8	264.5	22.02

Test	Temperature,				Heat Flow,			R-value
	Meter C	Climate C	Mean C	Thermopile C	Input, W	Metering Box W	Specimen W	m^2 K/W
1	37.2	11.3	24.2	-0.02	41.7	-0.1	41.6	3.725
2	37.1	11.5	24.3	-0.57	43.6	-2.0	41.6	3.725
3	37.2	10.6	23.9	0.48	39.6	1.7	41.3	3.728
4	35.9	-15.2	10.3	-0.03	78.2	-0.1	78.1	3.889
5	36.4	-14.1	11.1	0.48	75.8	1.7	77.5	3.880

We find excellent agreement between the test results generated between the two test apparatus; all five of the ASTM C 0236 experiments performed in the RGHB are within ± 0.2% of the ASTM C 0518 results from the heat flow meter apparatus. Even if our estimate of the thermal resistance of the polystyrene sheets were in error by 50%, the results from the two procedures would still agree to within 1.1%. The need to estimate the R-value of the polystyrene sheets does not appreciably compromise the results that are presented.

Table A2. A comparison of the ASTM C 236 (RGHB) and ASTM C 518 test results on specimens of the expanded polystyrene foam verification panel. The ASTM C 518 results are based on a linear regression of the results of the actual experiments as a function of temperature and are computed at the same mean temperature as the RGHB results.

Test	Mean Temperature	R-value, hr ft^2 F/Btu		% Difference, (C 236 - C 518)/C518
	F	ASTM C 236	ASTM C 518	
1	75.6	21.14	21.14	0.0
2	75.7	21.14	21.14	0.0
3	75.0	21.16	21.20	-0.2
4	50.6	22.07	22.07	0.0
5	52.0	22.07	22.01	0.1

Test	Mean Temperature	R-value, m^2 K/W		% Difference, (C 236 - C518)/C518
	C	ASTM C 236	ASTM C 518	
1	24.2	3.725	3.725	0.0
2	24.3	3.725	3.725	0.0
3	23.9	3.728	3.735	-0.2
4	10.3	3.889	3.889	0.0
5	11.1	3.880	3.878	0.1